

The profibrotic effects of MK-8617 on tubulointerstitial fibrosis mediated by the KLF5 regulating pathway

Zuo-Lin Li, Lin-Li Lv,¹ Bin Wang, Tao-Tao Tang, Ye Feng, Jing-Yuan Cao, Li-Qiong Jiang, Yan-Bei Sun, Hong Liu, Xiao-Liang Zhang, Kun-Ling Ma, Ri-Ning Tang, and Bi-Cheng Liu²

Institute of Nephrology, Zhong Da Hospital, Southeast University School of Medicine, Nanjing, China

ABSTRACT: The discovery of hypoxia-inducible factor (HIF)-prolyl hydroxylase inhibitor (PHI) has revolutionized the treatment strategy for renal anemia. However, the presence of multiple transcription targets of HIF raises safety concerns regarding HIF-PHI. Here, we explored the dose-dependent effect of MK-8617 (MK), a kind of HIF-PHI, on renal fibrosis. MK was administered by oral gavage to mice for 12 wk at doses of 1.5, 5, and 12.5 mg/kg. *In vitro*, the human proximal tubule epithelial cell line HK-2 was treated with increasing doses of MK administration. Transcriptome profiling was performed, and fibrogenesis was evaluated. The dose-dependent biphasic effects of MK on tubulointerstitial fibrosis (TIF) were observed in chronic kidney disease mice. Accordingly, high-dose MK treatment could significantly enhance TIF. Using RNA-sequencing, combined with *in vivo* and *in vitro* experiments, we found that Krüppel-like factor 5 (KLF5) expression level was significantly increased in the proximal tubular cells, which could be transcriptionally regulated by HIF-1 α with high-dose MK treatment but not low-dose MK. Furthermore, our study clarified that HIF-1 α -KLF5-TGF- β 1 signaling activation is the potential mechanism of high-dose MK-induced TIF, as knockdown of KLF5 reduced TIF *in vivo*. Collectively, our study demonstrates that high-dose MK treatment initiates TIF by activating HIF-1 α -KLF5-TGF- β 1 signaling. These findings provide novel insights into TIF induction by high-dose MK (HIF-PHI), suggesting that the safety dosage window needs to be emphasized in future clinical applications.—Li, Z.-L., Lv, L.-L., Wang, B., Tang, T.-T., Feng, Y., Cao, J.-Y., Jiang, L.-Q., Sun, Y.-B., Liu, H., Zhang, X.-L., Ma, K.-L., Tang, R.-N., Liu, B.-C. The profibrotic effects of MK-8617 on tubulointerstitial fibrosis mediated by the KLF5 regulating pathway. *FASEB J.* 33, 000–000 (2019). www.fasebj.org

KEY WORDS: HIF-PHI · tubulointerstitial fibrosis · HIF-1 · Krüppel-like factor 5 · TGF- β 1

The identification of oxygen-dependent prolyl hydroxylase (PH) domain (PHD) enzymes as regulators of hypoxia-inducible factor (HIF)-dependent erythropoiesis has led to the development of novel therapeutic agents for renal anemia (1, 2). The molecular mechanisms by which HIF-PH enzymes regulate the activity of HIF are well known. HIF is made up of 2 subunits: oxygen-responsive

HIF-1 α or HIF-2 α , and constitutive HIF- β . Under normoxic conditions, HIF- α , which is synthesized continuously, is hydroxylated by the HIF-PH enzymes. The resulting hydroxylated HIF- α is rapidly degraded by the von Hippel-Lindau-E3 ubiquitin ligase complex following ubiquitylation. When oxygen levels decrease, HIF-PH inhibition allows HIF- α translocation to the nucleus, where dimerization with HIF- β occurs, resulting in the activation of a large array of target hypoxia-responsive genes, including erythropoietin (EPO), and multiple genes involved in iron metabolism (3, 4). Thus, HIF-PH inhibitors (PHIs) primarily function by mimicking the hypoxia-driven expression of endogenous EPO and other associated genes.

Apart from EPO and multiple genes involved in iron metabolism, genes regulated by HIF also possess a broad spectrum of cellular functions and biologic processes (5). In fact, genes that are directly regulated by HIF and several hundred high-stringency HIF binding sites have been identified across the genome (6). HIF-PHI, an active inhibitor of HIF-PHDs, may affect the expression of genes with less-obvious roles in erythropoiesis and adaptation to hypoxia, which are involved in diverse pathways, including cell differentiation and immune responses (7).

ABBREVIATIONS: α -SMA, α -smooth muscle actin; AQP, aquaporin; BUN, blood urea nitrogen; CCK-8, Cell Counting Kit-8; ChIP, chromatin immunoprecipitation; CKD, chronic kidney disease; ECM, extracellular matrix; EPO, erythropoietin; Hb, hemoglobin; HIF, hypoxia-inducible factor; KLF5, Krüppel-like factor 5; Lv, lentivirus; MK, MK-8617; mpk, milligram per kilogram; NC, negative control; NCC, NaCl cotransporter; PH, prolyl hydroxylase; PHD, PH domain; PHI, PH inhibitor; SCr, serum creatinine; shRNA, short-hairpin RNA; siRNA, small interfering RNA; TEC, tubular epithelial cell; TIF, tubulointerstitial fibrosis

¹ Correspondence: Institute of Nephrology, Zhong Da Hospital, Southeast University School of Medicine, No. 87 Dingjiaqiao Rd., Gulou District, Nanjing 210000, China. E-mail: linlilv2000@hotmail.com

² Correspondence: Institute of Nephrology, Zhong Da Hospital, Southeast University School of Medicine, No. 87 Dingjiaqiao Rd., Gulou District, Nanjing 210000 China. E-mail: Liubc64@163.com

doi: 10.1096/fj.201901087RR

This article includes supplemental data. Please visit <http://www.fasebj.org> to obtain this information.

Therefore, the potential effects of HIF-PHIs on diverse pathways and the exact mechanisms are of major clinical and basic scientific concern.

Although HIF-PHIs were well tolerated in phase 2 trials and are currently in phase 3 clinical trials to treat patients with chronic kidney disease (CKD) and anemia (8,9), there are several safety concerns related to the potential non-erythropoietic effects due to repeated or persistent HIF activation. Moreover, other teams and ours demonstrated that HIF is involved in the regulation of a broad spectrum of matrix turnover, inflammation, and fibrogenesis (10–12). Thus, it is a considerable concern whether HIF activation induced by HIF-PHIs is beneficial or detrimental to the progression of CKD.

MK-8617 (MK), a recently identified, selective, orally bioavailable HIF-PHI, actively stimulates erythropoiesis (13). In this study, we evaluated the dose-dependent effects of MK on renal fibrosis. We demonstrated that high-dose MK treatment could significantly initiate tubulointerstitial fibrosis (TIF) by activating the HIF-1 α –Krüppel-like factor 5 (KLF5)–TGF- β 1 signaling pathway. This finding represents a previously unrecognized insight into the nonerythropoietic effects of HIF-PHIs.

MATERIALS AND METHODS

Animals

Experiments were performed with 6–8-wk-old, 20–22-g male C57BL/6 mice (Vital River Laboratory Animal Technology, Beijing, China). The mice were housed in a specific pathogen-free environment at the Animal Center of the Southeast University School of Medicine at optimal temperature with a 12-h light/dark cycle. The mice were also provided free access to water and standard mouse chow. The experimental procedures were approved by the Ethics Review Committees for Animal Experimentation of Southeast University. Subtotal nephrectomy (5/6 nephrectomy, 5/6Nx) model was performed as previously described by Yokoro *et al.* (14).

Lentiviral gene transfer *in vivo*

Lentiviruses (Lvs) expressing short-hairpin RNAs (shRNAs) targeting KLF5 (Lv-shKLF5) and negative control (NC) (Lv-shNC) were purchased from GenePharma (Shanghai, China). The shRNA targeting sequences were as follows: shKLF5, 5'-GTCCTCCAGTCCGATAAT-3', and shNC, 5'-TTCTCCG-AACGTGTCACGT-3'. Lv-mediated gene transfer in kidneys of 5/6Nx mice was performed by tail vein injection (5×10^8 TU/wk/mouse). Ten weeks postinjection, animals were euthanized, and tissues were rapidly collected.

HIF-PHI MK treatment

Twelve-week study with HIF-PHI MK in mice

MK was obtained from Selleck Chemicals (Houston, TX, USA). The 5/6Nx mice ($n = 7$ –9 per group) were dosed with vehicle [DMSO:PEG400:water (5:40:55, v/v/v)] or MK [1.5, 5, or 12.5 mg/kg (mpk) in vehicle] once daily for 12 wk. A group of age-matched, sham-treated control vehicle-administered mice ($n = 6$) were included in the experiments. In wk 0, 2, 4, 7, 10, and 12, blood samples were obtained *via* tail vein for hemoglobin (Hb)-level analyses (Supplemental Fig. S1).

Ten-week study with HIF-PHI MK in mice with Lv-shKLF5

The 5/6Nx mice with Lv-shKLF5 or Lv-shNC ($n = 4$ /group) were administered MK once daily for 10 wk (12.5 mpk in vehicle [DMSO:polyethylene glycol 400 (PEG400):water (5:40:55, v/v/v)]) (see Supplemental Fig. S2).

Plasma and urinary parameters

Serum and urinary creatinine, serum blood urea nitrogen (BUN), serum aspartate aminotransferase, serum alanine aminotransferase, and Hb levels were quantified using commercial kits (Jiancheng, Nanjing, China). Albumin concentrations in the collected urinary samples were measured using specific ELISA kits (Jiancheng) according to the manufacturer's instructions. Albumin excretion is presented as micrograms of albumin per milligram of creatinine. Serum EPO (Elabscience Biotechnology, Wuhan, China), VEGFA, hepcidin, and hypersensitive C-reactive protein (all from R&D Systems, Minneapolis, MN, USA) levels were measured using the commercially available ELISA kit according to the protocols.

Cell culture

The human proximal tubular epithelial cell (TEC) line HK-2 was purchased from American Type Culture Collection (Manassas, VA, USA). Cells were cultured in DMEM–Ham's F-12 medium (GE Healthcare, Waukesha, WI, USA) supplemented with 10% fetal bovine serum (Thermo Fisher Scientific, Waltham, MA, USA), penicillin (100 IU/ml), and streptomycin (100 μ g/ml; Thermo Fisher Scientific) in a humidified atmosphere of 5% CO₂ and 95% O₂ at 37°C.

Cell viability assay

Cell viability was examined by the Cell Counting Kit-8 (CCK-8) assay kit according to the manufacturer's instructions (ApexBio Technology, Houston, TX, USA). Briefly, the HK-2 cells were seeded in 96-well plates at a density of 5×10^4 cells/ml for 24 h and treated with various concentrations of MK (0, 50, 150, 500, 1000, and 2000 nM) for 24 h at 37°C, and then 10 μ l CCK-8 reagent was added to the medium and incubated for 2 h. The absorbance was detected at 450 nm.

Self-organizing map and bioinformatics analysis

We used RNA-sequencing to characterize the expression patterns of mRNA genes in HK-2 cells treated with MK. Self-organizing maps were intuitively used to analyze the structure and interrogate transcriptome data, as previously described by Kim *et al.* (15). The Kyoto Encyclopedia of Genes and Genomes database (KEGG; <https://www.genome.jp/kegg/kegg1.html>), a bioinformatics resource for the genome, was used to identify the significant pathways of the targeted genes.

Real-time quantitative PCR and small RNA interference studies

Frozen tissues or cells were analyzed for specific gene expression using real-time quantitative PCR. Briefly, total RNA was extracted using Trizol (Takara, Kyoto, Japan) and reverse transcribed using PrimeScript RT Reagent Kit (Takara). Real-time quantitative PCR was performed on a 7300 PCR System (Thermo Fisher Scientific). Primers for real-time quantitative PCR are

listed in Supplemental Table S1. Relative expression was normalized to glyceraldehyde 3-phosphate dehydrogenase levels. For small interfering RNA (siRNA)-mediated knockdown of KLF5 and HIF-2 α (Genepharma), HK-2 cells were transfected with 80 nM siRNA against human KLF5 (sense 5'-GCAGACUGCAGUGAAACAATT-3'; antisense 5'-UUGUUUCACUGCAGUCUGCTT-3') and human HIF-2 α (sense 5'-GCAUCAUGUGUGUCAACUAUU-3'; antisense 5'-AAUAGUUGACACA-CAUGAUGC-3'). A scramble sense control was used as the NC.

Western blotting

Western blotting was performed as previously described by Liu *et al.* (16). Anti-glyceraldehyde 3-phosphate dehydrogenase (CW0100M; Cwbio, Beijing, China), anti-HIF-1 α (ab2185), anti-HIF-2 α (ab199), anti- α -smooth muscle actin (α -SMA) (ab5694), anti-collagen-I (ab34710), anti-fibronectin (ab2413), anti-KLF5 (ab137676), and anti-TGF- β 1 (ab82486) (all from Abcam, Cambridge, MA, USA) antibodies were used.

Chromatin immunoprecipitation assay

Chromatin immunoprecipitation (ChIP) was performed with Simple ChIP Enzymatic ChIP Kit (magnetic beads) (9003; Cell Signaling Technology, Danvers, MA, USA) as previously described (12). Immunoprecipitation was performed with the antibody against HIF-1 α (ab2185; Abcam) or normal IgG as the NC. Precipitated DNA fragments were detected by PCR using primers specific for the promoter region of KLF5: forward 5'-CGGGCTCAAGTGATTCTCTCT-3', reverse 5'-GGAAACCCT-GTCCCTACTAAAAGTA-3'.

FISH

EPO transcripts were detected in formalin-fixed, paraffin-embedded kidney tissue sections using the RNAscope Multiplex Fluorescent Kit according to the manufacturer's instructions (Ribobio, Guangzhou, China). Fluorescent dye (FAM)-labeled locked nucleic acid oligonucleotide was used as a probe (Genepharma) to detect EPO mRNA; scramble locked nucleic acid was used as the control. Pictures were recorded using an Olympus FV-1000 confocal microscope (Olympus, Tokyo, Japan).

Immunofluorescence and immunohistochemistry

Immunofluorescence and immunohistochemistry were performed as previously described by Liu *et al.* (16). The primary antibodies anti-HIF-1 α (ab2185), anti-HIF-2 α (ab199), anti-collagen-I (ab34710), anti-KLF5 (ab137676), anti-KLF5 (sc-398470; Santa Cruz Biotechnology, Dallas, TX, USA), anti-aquaporin (AQP)1 (NB600-749; Novus, Centennial, CO, USA), anti-megalin (sc-515772; Santa Cruz Biotechnology), anti-NaCl cotransporter (NCC, AB3553; MilliporeSigma, Burlington, MA, USA), anti-AQP2 (NB110-74682; Novus), anti-TGF- β 1 (sc-52893; Santa Cruz Biotechnology), and anti-TGF- β 1 (ab82486) were used.

Statistical analyses

Data are presented as means \pm SEM. For experiments comparing 2 groups, the results were analyzed using the Student's *t* test or Mann-Whitney *U* test. When >2 groups were compared, a 1-way ANOVA followed by Dunnett's test or Bonferroni correction was employed to analyze the differences using SPSS v.20.0 (IBM

SPSS, Chicago, IL, USA). A 2-sided value of $P < 0.05$ was considered significant.

RESULTS

MK treatment has dose-dependent biphasic effects on Hb and kidney function

First, we analyzed changes of body weight and serological parameters after 12 wk of MK treatment (Supplemental Table S2). Interestingly, compared with vehicle-administered CKD mice, body weight was markedly decreased in mice dosed 12.5 mpk. EPO expression level was significantly increased in MK-treated mice, but this was markedly lower in mice administered 12.5 mpk than 5 mpk. Meanwhile, hepcidin levels significantly decreased in MK-treated mice compared with vehicle-administered CKD mice, with a significant increase in mice administered 12.5 mpk compared with those given 5 mpk. We also found that hypersensitive C-reactive protein and VEGFA levels were significantly increased in mice given 12.5 mpk compared with 5 mpk and vehicle-administered CKD mice. In addition, no changes in serum alanine aminotransferase and aspartate aminotransferase levels were observed.

Unexpectedly, we found that the spleen of mice administered 1.5 or 5 mpk MK appeared darker in color than those given 12.5 mpk MK and vehicle-administered CKD mice. Splenomegaly was observed in mice given 12.5 mpk MK (Supplemental Fig. S3A). Histologic analysis of spleens in mice administered 12.5 mpk MK revealed disruption in splenic architecture, reduced size of white pulp germinal centers, and a concomitant increase in red pulp (Supplemental Fig. S3B), suggesting that high-dose MK treatment might be harmful to spleen, a frequent site of extramedullary hematopoiesis in adult mice. To evaluate the effects of different MK doses on hematopoiesis, Hb levels were measured. Interestingly, before 7 wk, Hb levels increased significantly in a dose-dependent manner. After 7 wk, Hb continued to increase the doses of 1.5 or 5 mpk, and a significant decrease in Hb level with 12.5 mpk MK (Fig. 1A). For renal function, compared with vehicle-administered CKD mice, serum creatinine (SCr) and BUN were significantly decreased in mice given 1.5 or 5 mpk and increased in those administered 12.5 mpk MK (Fig. 1B). As expected, the same trend was seen for albuminuria. The data suggest that there were dose-dependent biphasic effects of MK on Hb and kidney function.

Non-cell-type-specific HIF-2 α and HIF-1 α stabilization by MK

We examined the effect of MK on HIF-2 α and HIF-1 α expression in kidney. Strikingly, Western blotting showed that MK could dose dependently stabilize HIF-2 α and HIF-1 α (Fig. 2A). Using immunohistochemistry analysis, we found that HIF-2 α and HIF-1 α were expressed in all cell types of the kidney (Fig. 2B, C), revealing no cell type-specific HIF-2 α and HIF-1 α stabilization by MK. As the HIF-dependent EPO gene is the target of HIF-PHI

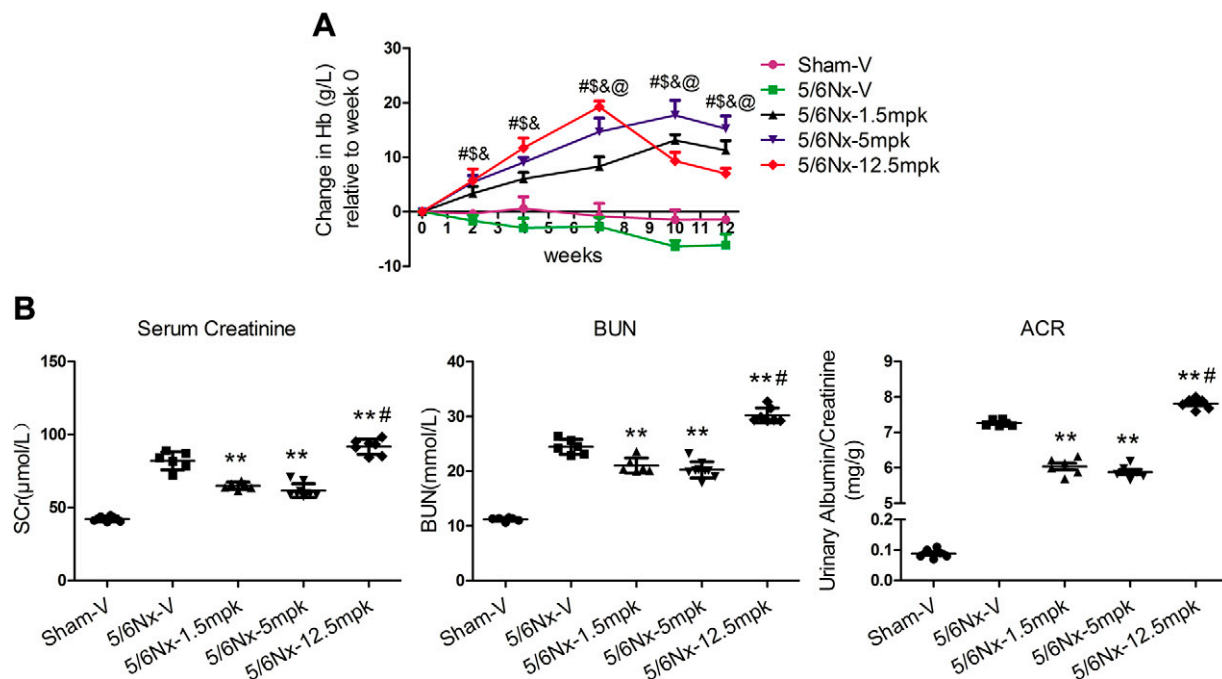


Figure 1. Dose-dependent biphasic effects of MK on Hb and renal function. A) Changes in Hb following an oral dose of MK to CKD mice for 12 wk; means \pm SEM ($n = 6-9$). $^{\#}P < 0.01$, 5/6Nx-1.5 mpk vs. 5/6Nx-V; $^{\$}P < 0.01$, 5/6Nx-5 mpk vs. 5/6Nx-V; $^{\&}P < 0.01$, 5/6Nx-12.5 mpk vs. 5/6Nx-V; $^{\textcircled{P}}P < 0.01$, 5/6Nx-12.5 mpk vs. 5/6Nx-5 mpk. B) SCr, BUN, and urinary albumin/creatinine (ACR) levels were assessed. $^{**}P < 0.01$ vs. 5/6Nx-V, $^{\#}P < 0.01$ vs. 5/6Nx-5 mpk (means \pm SEM; $n = 6-9$).

treatment in anemia, EPO gene levels were analyzed. Real-time PCR analysis shows that EPO mRNA expression was significantly increased in the kidney of mice administered 1.5 or 5 mpk MK and was significantly lower in the kidney of mice given 12.5 mpk compared with 5 mpk MK (Fig. 2D). Furthermore, the FISH study indicates that renal interstitial cells were the sites of EPO production (Fig. 2E).

MK has dose-dependent biphasic effects on TIF *in vivo*

Notably, as detected by Masson staining, TIF was significantly attenuated in mice administered 1.5 or 5 mpk MK, whereas it was markedly increased in mice with the 12.5-mpk dosing compared with the vehicle-administered CKD mice (Fig. 3A). Furthermore, we analyzed transcript and protein levels of α -SMA, collagen-I, and fibronectin, which have defined roles in TIF. Compared with the vehicle-administered CKD mice, α -SMA, collagen-I, and fibronectin mRNA were significantly decreased in the kidney of mice given 1.5 or 5 mpk MK and markedly increased in mice administered 12.5 mpk (Fig. 3B). The protein expression pattern associated with TIF was also confirmed by Western blotting (Fig. 3C). By using collagen-I antibody for immunofluorescence, fibrosis was found to be predominantly located in the tubulointerstitium (Fig. 3D).

High-dose MK induces fibrogenesis in TECs

Convincing evidence indicates that TECs as a driving force contributes to interstitial inflammation and fibrosis (17).

To investigate the potential fibrogenic effect of MK on the TEC, a human proximal TEC line (HK-2) was used. First, a cell viability assay was performed in HK-2 cells with MK treatment at increasing concentrations from 0 to 2000 nM for 24 h using a CCK-8 assay. MK treatment did not decrease cell viability of HK-2 cells at the concentrations within 1000 nM. However, decreased cell viability was observed in HK-2 cells treated with MK at the concentration of 2000 nM (Supplemental Fig. S4). These results indicate that no obvious cellular toxicity on HK-2 cells was within 1000 nM. Thus, the HK-2 cells were administrated with MK at increasing concentrations from 0 to 1000 nM. Western blotting showed that MK could dose dependently stabilize HIF-2 α and HIF-1 α (Fig. 4A). Interestingly, as indicated by the transcript and protein levels of α -SMA, collagen-I, and fibronectin, fibrogenesis was promoted in HK-2 cells with doses of 500 and 1000 nM MK (Fig. 4B, C). Furthermore, to prove that the profibrotic effect of high-dose MK treatment depended on the HIF-1 α but not HIF-2 α activation, we knocked down HIF-2 α expression by siRNA interference in HK-2 cells before administration of MK. Interestingly, as indicated by the protein levels of α -SMA and collagen-I, the fibrogenic effect of high-dose MK treatment depended on the HIF-1 α but not HIF-2 α activation (Fig. 4D). It thus seems that fibrogenesis of TEC could be induced by high-dose MK.

Transcriptional regulation of KLF5 by HIF-1 α plays a central role in TIF

To investigate the exact mechanisms of the fibrogenic effect induced by MK, a genome-wide gene expression analysis was performed in MK-stimulated HK-2 cells at

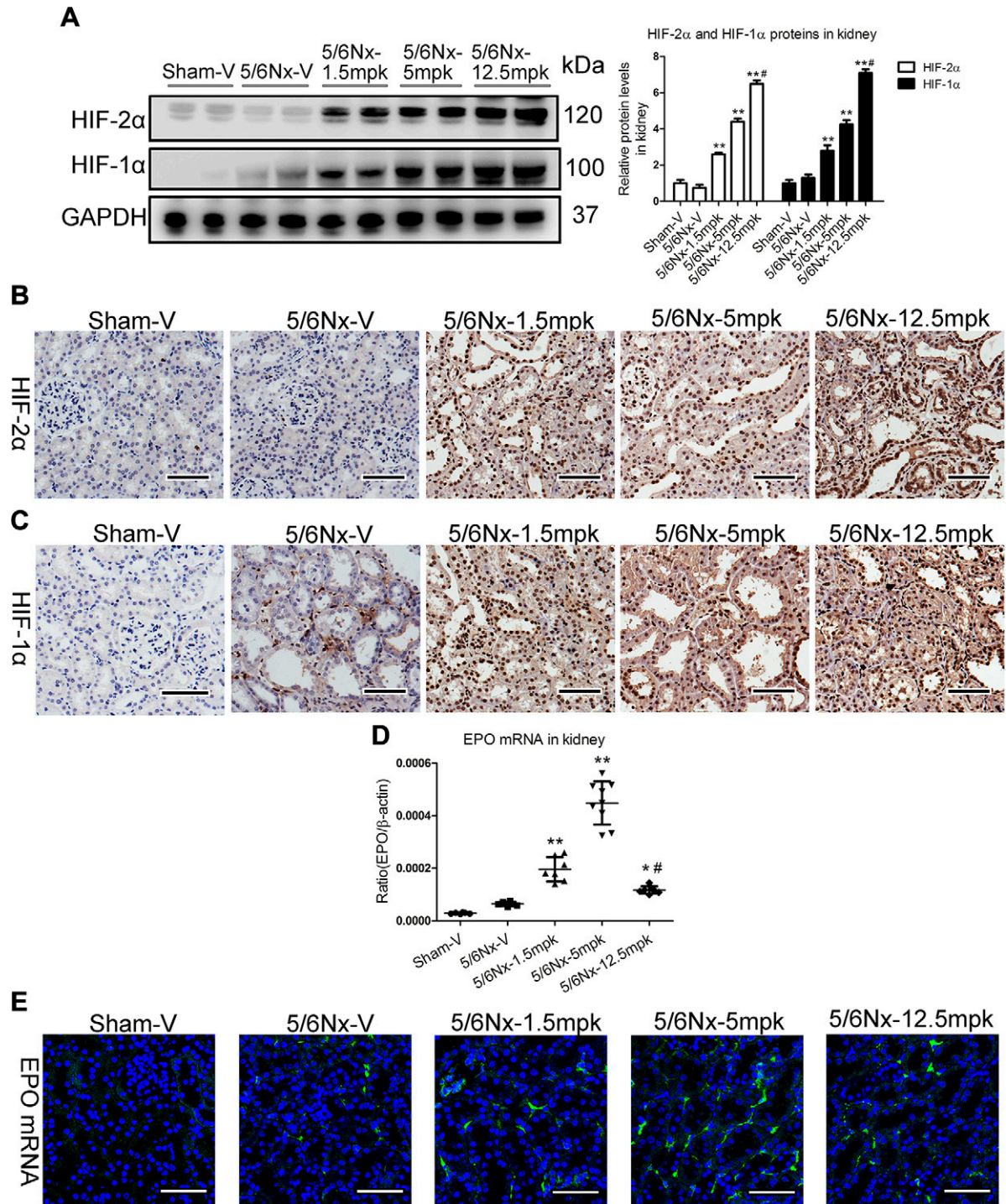


Figure 2. Non-cell-type-specific HIF-2 α and HIF-1 α stabilization by MK. *A*) Western blotting results of HIF-2 α and HIF-1 α expression in the cortex of kidney. GAPDH, glyceraldehyde 3-phosphate dehydrogenase. *B*, *C*) Representative results of HIF-2 α (*B*) and HIF-1 α (*C*) immunostaining. Scale bars, 50 μ m. *D*) EPO mRNA expression by real-time PCR. *E*) Representative images of EPO mRNA detection by RNA *in situ* hybridization. Scale bars, 50 μ m. Data are presented as the means \pm SEM of 6–9 mice. * P < 0.05, ** P < 0.01 vs. 5/6Nx-V, # P < 0.01 vs. 5/6Nx-5 mpk.

low (50 nM) and high (1000 nM) doses. To identify the inherent transcriptome features in TEC with MK administration, a self-organizing map was applied for feature selection. To facilitate direct comparison between different MK treatment doses, component plane presentations were used to display sample-specific transcriptome changes (Supplemental Fig. S5A). The topological relationships of 7

clusters are shown in Supplemental Fig. S5B. Genes within the same cluster displayed highly similar expression patterns, suggesting that they may share common features. As genes highly expressed in the high-dose MK group, we collected genes differentially expressed (false-discovery rate < 0.05) in cluster 4 (Fig. 5A) and performed pathway analysis to determine whether they shared regulatory

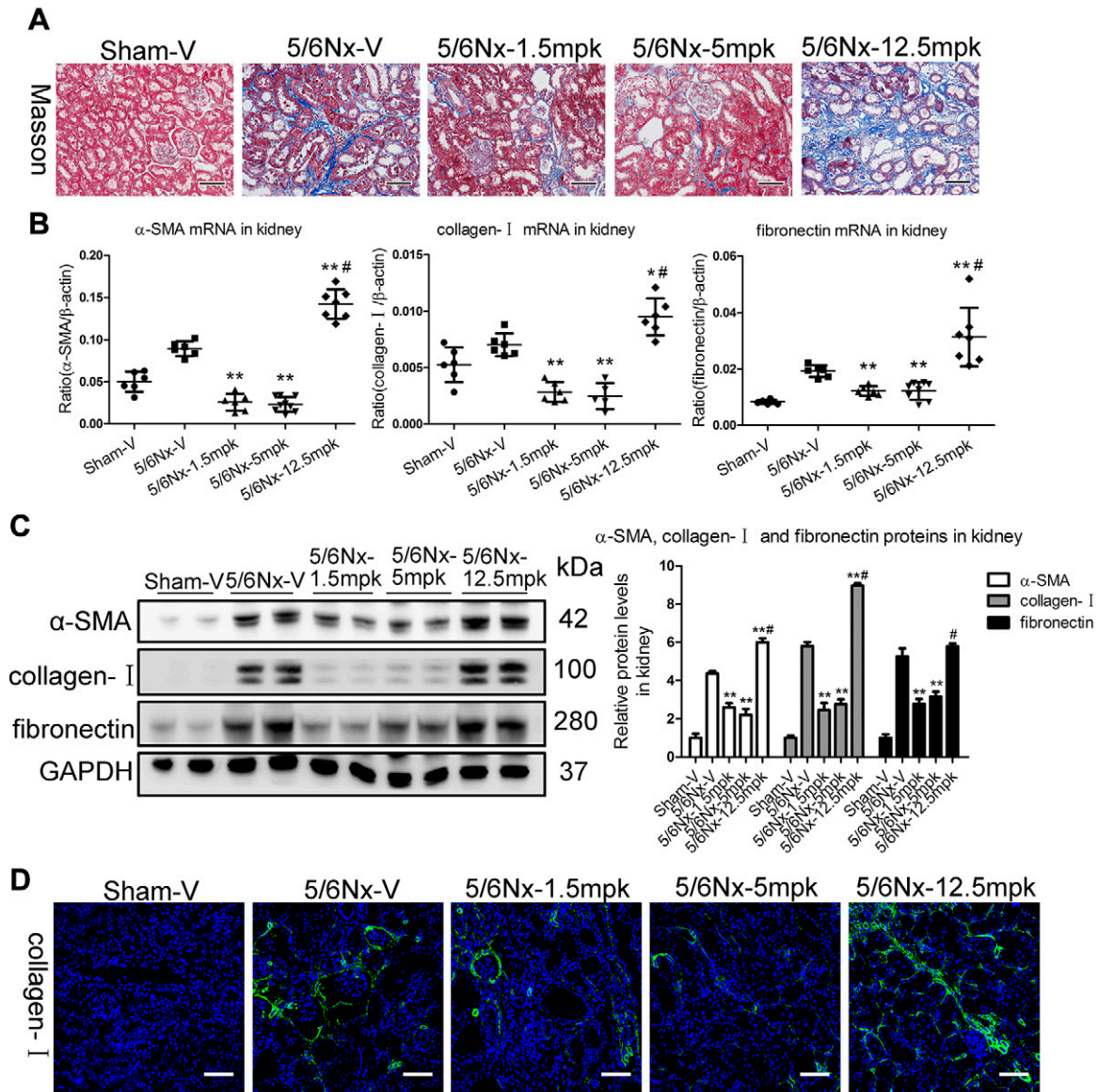


Figure 3. Dose-dependent biphasic effects of MK on TIF *in vivo*. **A**) Representative images of Masson staining of the kidney. Scale bars, 100 μ m. **B, C**) α -SMA, collagen-I, and fibronectin mRNA and protein expression in the cortex of kidney, as determined by real-time PCR (**B**) and Western blotting (**C**). GAPDH, glyceraldehyde 3-phosphate dehydrogenase. **D**) Representative images of collagen-I immunostaining. Scale bars, 100 μ m. Data are presented as the means \pm SEM of 6–9 mice. * P < 0.05, ** P < 0.01 vs. 5/6Nx-V, # P < 0.01 vs. 5/6Nx-5 mpk.

features of fibrogenesis. As shown in Supplemental Fig. S5C, the significant pathways in this cluster include those associated with fibrogenesis, suggesting that high-dose MK treatment may have a potential fibrogenic effect on TECs.

Intriguingly, KLF5 expression appeared to be markedly up-regulated in high-dose MK-stimulated HK-2 cells (Fig. 5A). Thus, genome-wide sequencing analysis data were validated both *in vivo* and *in vitro* using real-time quantitative PCR. We found that KLF5 mRNA level was significantly increased in the kidney of mice dosed at 12.5 mpk (Supplemental Fig. 5D), and its protein expression pattern was also confirmed by Western blotting (Fig. 5B). Immunofluorescence analysis further revealed that in normal kidneys, KLF5 was expressed in some specific cells, including the collecting ducts and glomerular cells, but not

in proximal and distal tubules. However, in the kidney of mice administered 12.5 mpk MK, KLF5 was expressed in all tubular cells, including the proximal and distal tubules (Fig. 5C), suggesting that KLF5 expression in the proximal and distal tubules might contribute to TIF. More interestingly, after 1000 nM MK administration *in vitro*, KLF5 mRNA and protein expression were significantly up-regulated (Supplemental Fig. S5E, F). These data indicate that KLF5 might be involved in TIF induction by high-dose MK.

To determine the exact mechanisms of KLF5 up-regulation induced by MK, *in silico* analysis was employed. Computational transcription factor-binding site prediction in the promoter region suggested that HIF-1 α may transcriptionally regulate KLF5 (Supplemental Fig. S6). Thus, we performed chromatin immunoprecipitation

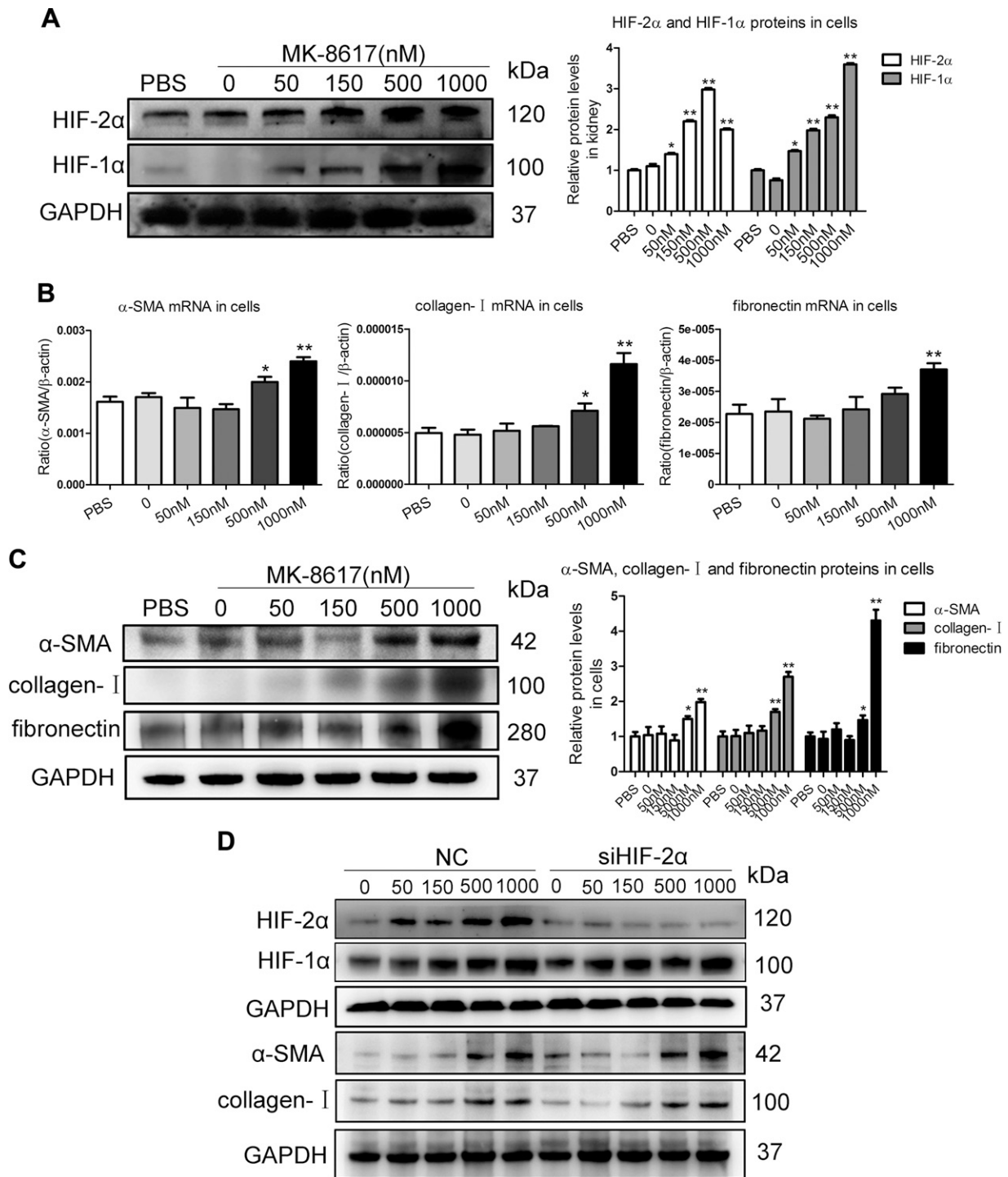


Figure 4. Fibrogenic effects of MK in TECs. *A*) Western blotting results of HIF-2 α and HIF-1 α expression in HK-2 cells treated with MK for 24 h. *B, C*) Effects of different doses of MK on α -SMA, collagen-I, and fibronectin mRNA (18 h) and protein (24 h) in HK-2 cells, as determined by real-time PCR (*B*) and Western blotting (*C*). Data are presented as means \pm SEM of 3 independent experiments. * $P < 0.05$, ** $P < 0.01$ vs. vehicle. *D*) Western blotting results of α -SMA and collagen-I expression in HK-2 cells with MK treatment after HIF-2 α siRNA interference ($n = 3$). GAPDH, glyceraldehyde 3-phosphate dehydrogenase.

assays to confirm the presence of HIF-1 α at the promoter region of KLF5. As expected, HIF-1 α did not bind to the KLF5 promoter under basal conditions and low-dose (50 nM) MK treatment, but HIF-1 α binding could be enriched on this promoter by high-dose (1000 nM) MK administration to HK-2 cells (Fig. 5D), demonstrating the direct interaction between HIF-1 α and KLF5 in response to

high-dose MK. HIF-1 α is therefore a strong positive regulator of the KLF5 gene during high-dose MK treatment.

To further characterize a possible functional effect of KLF5 on fibrogenesis in TEC, KLF5 knockdown experiments using siRNA-targeted KLF5 were performed. KLF5 protein level was significantly down-regulated after KLF5 siRNA transfection in MK (1000 nM)-treated HK-2 cells.

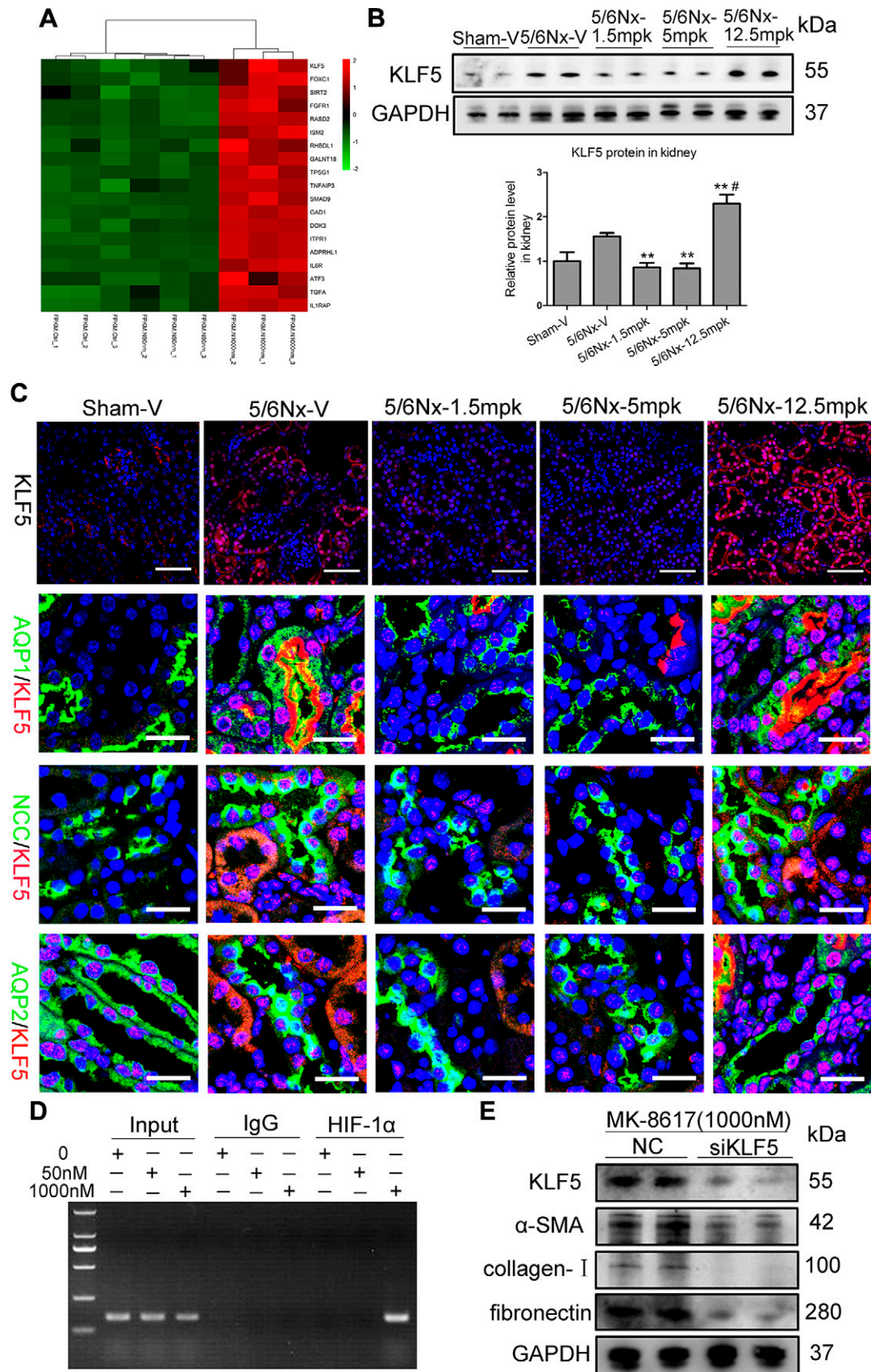


Figure 5. Transcriptional regulation of KLF5 by HIF-1 plays a key role in TIF. **A**) Hierarchical clustering shows distinct mRNA expression profiling among groups. The red and green shades indicate the expression above and below the relative expression, respectively, across all samples. **B**) KLF5 protein expression in the kidney cortex after MK treatment. $**P < 0.01$ vs. 5/6Nx-V, $\#P < 0.01$ vs. 5/6Nx-5 mpk. (Means \pm SEM; $n = 6-9$). **C**) Representative data of KLF5 immunostaining in kidney. Scale bars, 100 (continued on next page)

Meanwhile, knockdown of KLF5 markedly diminished the increase in α -SMA, collagen-I, and fibronectin (Fig. 5E). These data further indicate that KLF5 transcriptionally regulated by HIF-1 α contributes to TIF during high-dose MK treatment.

KLF5 stimulates fibrogenesis by up-regulating TGF- β 1

Convincing evidence has shown that TGF- β , a critical initiator in tissue fibrosis due to its regulation of the production of extracellular matrix (ECM) components (18), including various types of collagen and fibronectin, lies downstream of KLF5 (19). To examine the potential role of the KLF5–TGF- β 1 axis in TIF, the effect of MK on TGF- β 1 expression *in vivo* was examined. Interestingly, real-time PCR results show that TGF- β 1 mRNA was significantly increased in the kidney of mice administered at 12.5 mpk (Supplemental Fig. S7), and its protein expression pattern was confirmed by Western blotting (Fig. 6A). Immunohistochemistry and immunofluorescence analysis further revealed that, in the proximal and distal tubules of mice administered 12.5 mpk MK treatment, TGF- β 1 expression level was significantly increased (Fig. 6B). Furthermore, an increasing expression of TGF- β 1 protein with 500 and 1000 nM MK treatment was observed *in vitro* (Fig. 6C). To examine the potential regulatory role of KLF5 in TGF- β 1, we performed KLF5 knockdown experiments using siRNA against KLF5. Strikingly, compared with HK-2 cells transfected with nonspecific NC, KLF5 knockdown significantly attenuated TGF- β 1 protein up-regulation in HK-2 cells with high-dose (1000 nM) MK treatment (Fig. 6D). Thus, KLF5–TGF- β 1 axis activation promotes TIF during high-dose MK treatment.

KLF5 activation induced by high-dose MK promotes TIF in CKD mice

To confirm the functional fibrogenic effects of KLF5 on kidney *in vivo*, KLF5 knockdown in mice was performed using Lv-shKLF5. Notably, renal knockdown efficiency was evidenced (Supplemental Fig. S8A, B). MK (12.5 mpk) was administered to Lv-shKLF5 and Lv-shNC-injected CKD mice. Interestingly, Lv-shKLF5-injected mice developed redness in their snouts and paws (Supplemental Fig. S8C), suggesting potential anemia correction and renoprotection. Indeed, the decreased Hb and EPO mRNA levels were significantly diminished in Lv-shKLF5-injected mice (Supplemental Fig. S8D, E). Meanwhile, the

injuries in kidney due to high-dose MK, as determined by biochemical measurements (SCr and BUN) and periodic acid-Schiff and Masson staining, were diminished by Lv-shKLF5 injection (Fig. 7A–C). Interestingly, as shown in Fig. 7D, E, Lv-shKLF5 largely abrogated the fibrogenic effect of MK, as evidenced by the transcript and protein levels of TGF- β 1, α -SMA, collagen-I, and fibronectin. Meanwhile, these results were also confirmed by TGF- β 1 and collagen-I immunostaining (Fig. 7E, G), further supporting the essential role of the KLF5–TGF- β 1 axis in mediating TIF during MK treatment. These results demonstrate that the critical role of KLF5 in TIF is induced by high-dose MK treatment.

DISCUSSION

Current findings suggest that HIF-PHIs, which are in trials for treatment of anemia caused by renal insufficiency, are clinically effective and well tolerated in phase 2 clinical trials (2, 8, 9, 20, 21). However, whether different doses of HIF-PHI treatment could alter the progression of kidney disease is uncertain. Here, we demonstrate that there are dose-dependent biphasic effects of MK treatment on TIF in CKD. Accordingly, high-dose MK treatment could significantly enhance TIF. We demonstrated that KLF5 expression was significantly increased in the proximal tubular cells, which could be transcriptionally regulated by HIF-1 α with high-dose MK treatment. Moreover, we clarified that HIF-1 α –KLF5–TGF- β 1 signaling activation represents a novel molecular mechanism in which high-dose MK treatment promotes TIF. These findings provide unique insights into the interdigitating mechanisms of HIF-PHI treatment in the kidney.

Defining the dose windows of HIF-PHI treatment with the greatest degree of accuracy is important, but unfortunately, this has yet to be performed. Previous studies have suggested that HIF activation over long periods promotes renal fibrosis (10, 22, 23). However, the effect of different HIF-PHI treatment doses on CKD progression has not been addressed. In the present study, we found that there were dose-dependent biphasic effects of MK on CKD progression. Namely, treatment with low- and middle-dose MK would be beneficial to kidney function *via* TIF amelioration. Paradoxically, high-dose MK treatment would aggravate the decline in kidney function by promoting TIF. Thus, the opposing effects of different MK treatment doses on TIF raise an important issue regarding drugs that target the HIF-mediated oxygen-sensing and response system.

μ m. Representative immunofluorescence double staining of AQP1 (green, proximal tubules), NCC (green, distal tubules), AQP2 (green, collecting ducts), and KLF5 (red) in kidneys of mice. Scale bars, 40 μ m. D) Chromatin immunoprecipitation assays show binding of HIF-1 to KLF5 promoter, which is mediated by MK stimulation (1000 nM for 18 h). E) Effect of KLF5 knockdown using KLF5 siRNA on protein expression of α -SMA, collagen I, and fibronectin in HK-2 cells treated with MK for 24 h, as determined by Western blotting. ADPRHL1, ADP-ribosylhydrolase-like 1; ATF3, activating transcription factor 3; DOK3, docking protein 3; FGFR1, fibroblast growth factor receptor 1; FOXO1, Forkhead box C1; GAD1, glutamate decarboxylase 1; GALNT18, polypeptide N-acetylgalactosaminyltransferase 18; GAPDH, glyceraldehyde 3-phosphate dehydrogenase; IL1RAP, interleukin 1 receptor accessory protein; IL6R, interleukin 6 receptor; ISM2, isthmin 2; ITPR1, inositol 1,4,5-trisphosphate receptor type 1; RASD2, RASD family member 2; RHBDL1, rhomboid-like 1; SIRT2, sirtuin 2; TGFA, TGF α ; TNFAIP3, TNF α -induced protein 3; SMAD9, SMAD family member 9; TSPG1, trypsin γ 1. ** P < 0.01 *vs.* vehicle (means \pm SEM; n = 3).

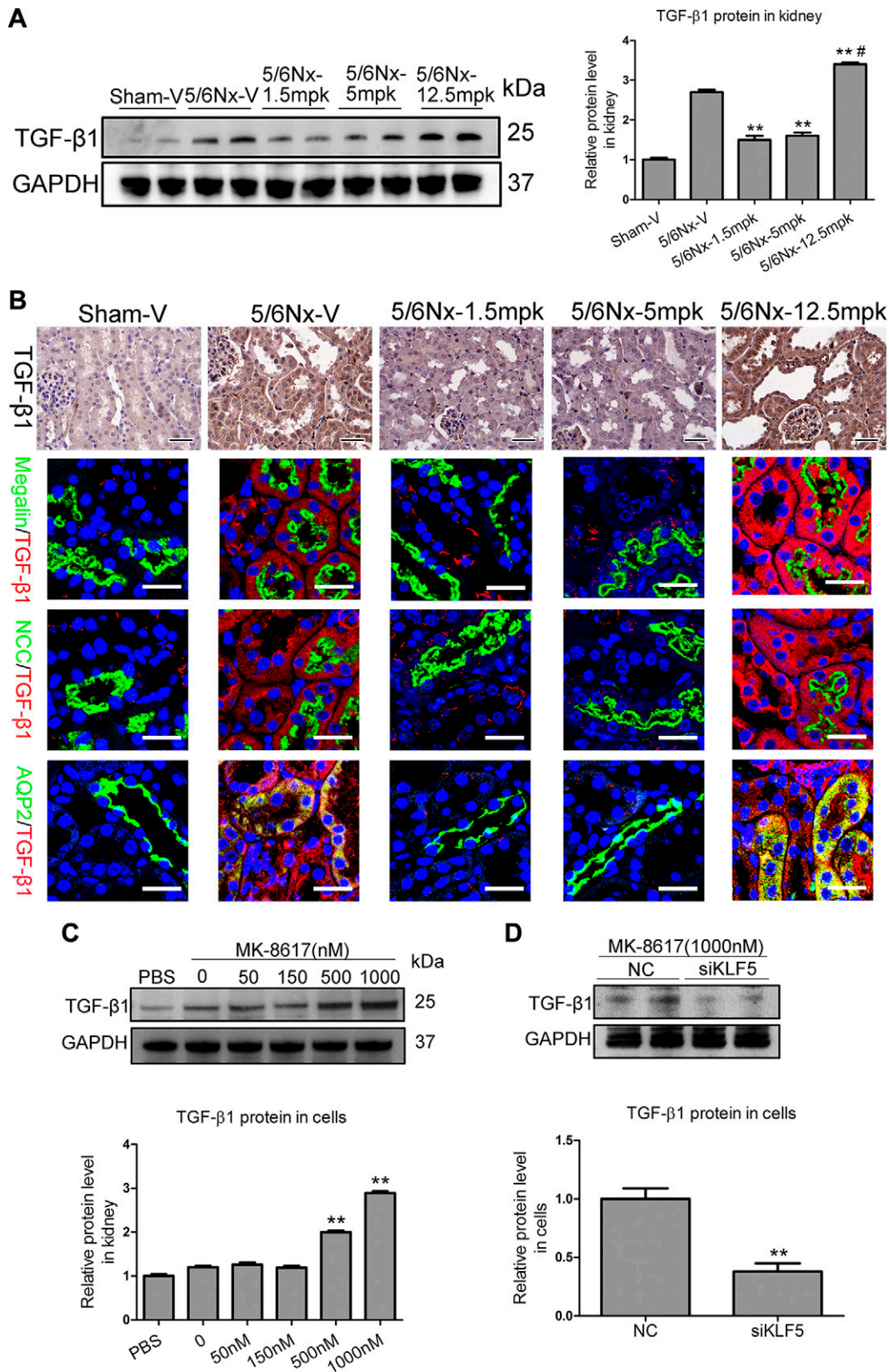


Figure 6. KLF5 stimulates fibrogenesis *via* TGF-β1. *A*) Representative Western blotting results of TGF-β1 in the kidney after MK treatment. * $P < 0.05$, ** $P < 0.01$ vs. 5/6Nx-V, # $P < 0.01$ vs. 5/6Nx-5 mpk (means \pm SEM; $n = 6-9$). *B*) Representative data for TGF-β1 immunostaining in kidney after MK treatment. Scale bars, 50 μ m. Representative immunofluorescence double staining of Megalin (green, proximal tubules), NCC (green, distal tubules), AQP2 (green, collecting ducts), and TGF-β1 (red) in kidneys of mice. Scale bars, 40 μ m. *C*) Effect of MK on TGF-β1 protein (24 h) in HK-2 cells. ** $P < 0.01$ vs. vehicle (means \pm SEM; $n = 3$). *D*) Effect of KLF5 knockdown using KLF5 siRNA on TGF-β1 protein expression. GAPDH, glyceraldehyde 3-phosphate dehydrogenase. ** $P < 0.01$ vs. vehicle (means \pm SEM; $n = 3$).

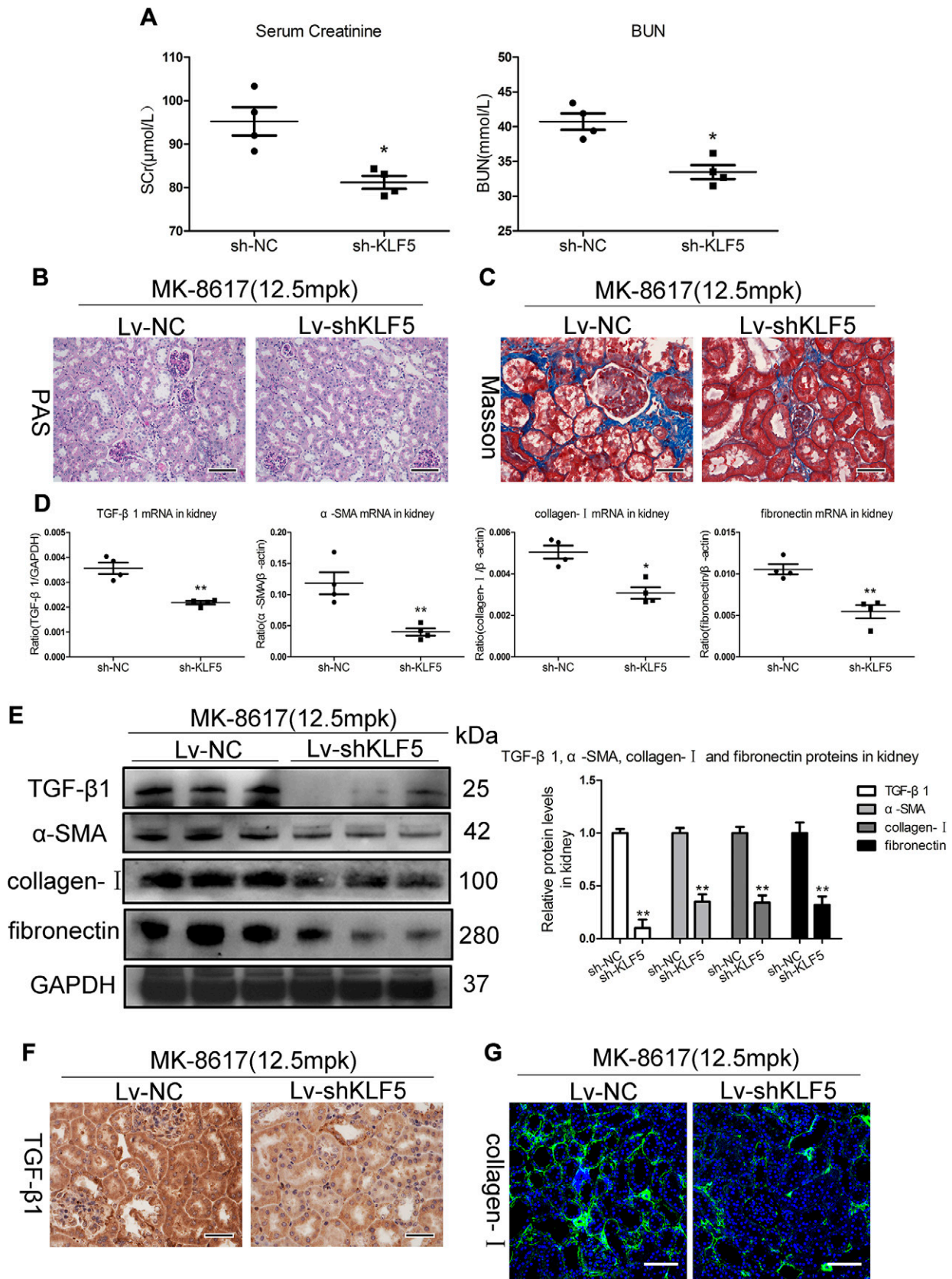


Figure 7. KLF5-dependent fibrogenic effects of high-dose MK *in vivo*. *A*) SCr and BUN levels were assessed. *B*) Representative changes in periodic acid-Schiff (PAS) staining. Scale bars, 100 μm. *C*) Representative changes in Masson staining. Scale bars, 50 μm. *D, E*) mRNA and protein (TGF-β1, α-SMA, collagen-I, and fibronectin) expression in the cortex of kidney, as determined by real-time PCR (*D*) and Western blotting (*E*). *F*) Representative immunohistochemical staining of TGF-β1. Scale bars, 50 μm. *G*) Representative immunofluorescence staining of collagen-I. Scale bars, 100 μm. GAPDH, glyceraldehyde 3-phosphate dehydrogenase. Data are presented as means ± SEM of 4 mice. **P* < 0.05, ***P* < 0.01 vs. Lv-NC.

Increasing evidence indicates that TECs are especially vulnerable to damage and often localize at the epicenter of kidney injury. After severe or recurrent injury, TECs undergo changes in structure, phenotype, and profibrotic factor expression (24, 25). In this study, we found that treatment with high-dose MK significantly enhanced TIF. Using RNA-sequencing combined with *in vivo* and *in vitro* experiments, we identified that abnormal activation of tubular KLF5, which was transcriptionally regulated by HIF-1 α , was demonstrated to be involved in TIF due to enhanced expression of ECM. The pathologic effects of tubular-activated KLF5 on TIF were also demonstrated by KLF5 knockdown *in vitro* and *in vivo*. Interestingly, Chen *et al.* (26) demonstrated that KLF5 could be expressed in proximal tubular cells in fibrotic kidneys. In addition, there is strong evidence that KLF5 is a crucial determinant of cellular response to injury in tissue remodeling (27). Thus, tubular KLF5 activation represents a novel mechanism for high-dose MK-induced TIF. However, the precise regulatory pathway for this effect has not been described.

KLF5 has a critical role in phenotypic modulation and tissue remodeling by controlling the expression of various growth factors (*e.g.*, TGF- β 1) (19). TGF- β 1 is a well-known primary factor that drives fibrosis in most forms of CKD. Inhibition of TGF- β 1 or its downstream signaling pathway substantially limits renal fibrosis in a wide range of disease models by regulating the balance between ECM production and degradation (28, 29). Therefore, we hypothesized that tubular KLF5 activation could modulate TIF by regulating TGF- β 1 in MK treatment. As expected, KLF5 transcriptionally regulated by HIF-1 α induced TGF- β 1 up-regulation in tubule, leading to TIF. Moreover, the pathologic effects of KLF5-induced TGF- β 1 in TIF were demonstrated *in vivo*. Interestingly, Takeda *et al.* (30) indicated that KLF5 was a key contributor to cardiac fibrosis due to the production of ECM proteins and a variety of paracrine factors. Therefore, KLF5-TGF- β 1 is a critical regulator of high-dose MK treatment-induced TIF.

One of the major clinical and rather basic interests is why the erythropoietic effects were attenuated in mice with the high dose of MK. It has been well known that the EPO in kidney is mainly produced by renal EPO-producing cells, which are predominantly located in the tubulointerstitium (31). We found that TIF was significantly increased, accompanying the reduced mRNA level

of EPO under the treatment of high-dose MK. Interestingly, Souma *et al.* (32) revealed that the majority of myofibroblasts, which play a central role in renal fibrosis, are derived from EPO-producing cells. Therefore, fibrogenesis of renal EPO-producing cells probably provides an explanation about why erythropoietic effects were attenuated in mice with the high dose of MK. Furthermore, we demonstrated that lessening TIF by knockdown KLF5 could markedly diminish the reduced erythropoietic effects of high-dose MK. In addition, the dysregulation of iron metabolism and inflammatory state in CKD mice with a high dose of MK (increased hepcidin levels and elevated inflammatory factors), which contributes to inhibiting duodenal iron absorption and sequestering iron in macrophages, decreasing availability of iron for erythropoiesis (33), could also provide a reasonable explanation. Thus, the profibrotic role and dysregulation of iron metabolism induced by high-dose MK may explain the potential mechanisms for its attenuated erythropoietic effects.

Another interest involves understanding how to avoid the potential harmful effects of HIF-PHI treatment. In clinical trials, HIF-PHI administration 2 or 3 times weekly was sufficient to effectively stimulate erythropoiesis (34, 35). As kidney and liver are likely to be the main targets, oral medication should be efficiently and precisely delivered to the desired site of action, and inhibition of PHDs needs to be only partial and intermittent to increase EPO production. Judicious selection of a low-dose, infrequent administration and monitoring of Hb levels could, therefore, increase the safety margin and avoid other non-erythropoietic effects, whose quality and extent may be determined by the degree and duration of HIF activation. In addition to HIF-mediated adverse effects, HIF-PHIs have the potential to interfere with cell signaling pathways involving proline hydroxylation of non-HIF signaling molecules and epigenetic gene regulation (36). These other potential effects on nonerythropoiesis of HIF-PHI should be addressed in future studies.

In addition, we also found that MK seemed to enhance glomerular expression of HIF- α . However, the roles of glomerular expression of HIF- α in EPO production and renal fibrosis were largely unclear. Previously, Paliege *et al.* (37) reported that HIF-2 α -expressing interstitial fibroblasts are the only renal cells that express EPO under HIF stabilizer. However, Gerl *et al.* (38) had demonstrated that

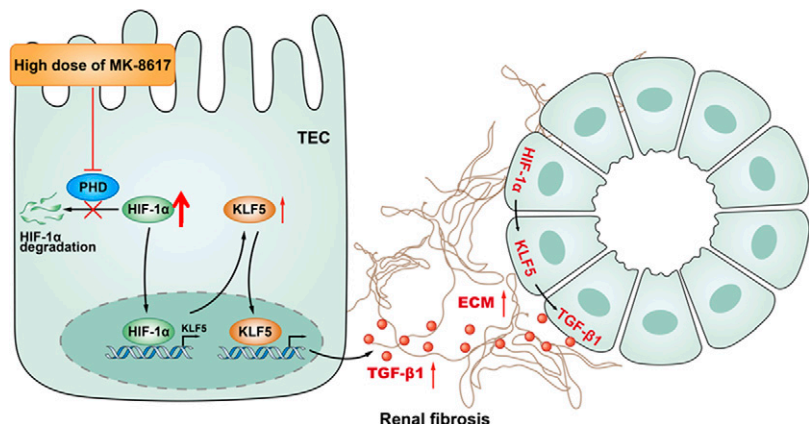


Figure 8. Schematic diagrams showing the proposed mechanism of high-dose MK treatment-mediated TIF. During high-dose HIF-PHI MK treatment for anemia, tubular KLF5 transcriptionally regulated by HIF-1 α promotes TIF *via* TGF- β 1.

inducible deletion of von Hippel-Lindau (vHL) in glomerular endothelial and mesangial cells markedly increased glomerular EPO mRNA expression levels, plasma EPO concentrations, and hematocrit values, suggesting that glomerular expression of HIF- α may be involved in the anemia correction. As for the effects of glomerular expression of HIF- α on renal fibrosis, it may mainly depend on cellular and experimental context. Convincing evidence indicates that renal function after acute and chronic kidney injury is independent of HIF-1 α in glomerular endothelial cells (39). However, elevated endothelial HIF-1 α is essential to initiate glomerular injury and progression to renal fibrosis under hypertensive CKD (40). For hypoxic renal injury, HIF-1 α stabilization in podocytes could induce glomerular endothelial cells' survival (41), whereas activation of HIF- α in mesangial cells promoted glomerulosclerosis (11, 42). Thus, HIF- α is a pivotal regulator of kidney fibrosis under various pathologic conditions. However, it remains controversial whether glomerular expression of HIF- α promotes or antagonizes renal fibrosis.

In summary, a very important potential effect of HIF-PHI on the kidney has been demonstrated definitively (Fig. 8). During high-dose MK (HIF-PHI) treatment for renal anemia, tubular KLF5, which is transcriptionally regulated by HIF-1 α , promotes TIF *via* TGF- β 1. These findings provide unique insights into the interdigitating mechanisms of HIF-PHI treatment in the kidney, highly suggesting that the safety dosage window needs to be emphasized in future clinical applications. FJ

ACKNOWLEDGMENTS

The authors thank Fang-Yuan Qian (Southeast University School of Medicine) for the valuable comments and suggestions in histological analysis. The authors also thank Chen-Chen Zhang (Southeast University School of Medicine) for confocal image acquisition and valuable technical support. This study is supported by the National Natural Scientific Foundation of China (Grants 81720108007, 81470922, 31671194, 81470997, and 81670696) and National Key Research and Development Program of China (2018YFC1314002). The authors declare no conflicts of interest.

AUTHOR CONTRIBUTIONS

Z.-L. Li, L.-L. Lv, and B.-C. Liu, designed research, performed the experiments, analyzed data, and wrote and edited the paper. B. Wang, T.-T. Tang, Y. Feng, J.-Y. Cao, L.-Q. Jiang, and Y.-B. Sun performed research and analyzed data; and H. Liu, X.-L. Zhang, K.-L. Ma, and R.-N. Tang analyzed data, reviewed and edited the manuscript.

REFERENCES

1. Koury, M. J., and Haase, V. H. (2015) Anaemia in kidney disease: harnessing hypoxia responses for therapy. *Nat. Rev. Nephrol.* **11**, 394–410
2. Sugahara, M., Tanaka, T., and Nangaku, M. (2017) Prolyl hydroxylase domain inhibitors as a novel therapeutic approach against anemia in chronic kidney disease. *Kidney Int.* **92**, 306–312

3. Jaakkola, P., Mole, D. R., Tian, Y. M., Wilson, M. I., Gielbert, J., Gaskell, S. J., von Kriegsheim, A., Hebestreit, H. F., Mukherji, M., Schofield, C. J., Maxwell, P. H., Pugh, C. W., and Ratcliffe, P. J. (2001) Targeting of HIF- α to the von Hippel-Lindau ubiquitylation complex by O₂-regulated prolyl hydroxylation. *Science* **292**, 468–472
4. Haase, V. H. (2013) Regulation of erythropoiesis by hypoxia-inducible factors. *Blood Rev.* **27**, 41–53
5. Semenza, G. L. (2019) Pharmacologic targeting of hypoxia-inducible factors. *Annu. Rev. Pharmacol. Toxicol.* **59**, 379–403
6. Schödel, J., Oikonomopoulos, S., Ragoussis, J., Pugh, C. W., Ratcliffe, P. J., and Mole, D. R. (2011) High-resolution genome-wide mapping of HIF-binding sites by ChIP-seq. *Blood* **117**, e207–e217
7. Maxwell, P. H., and Eckardt, K. U. (2016) HIF prolyl hydroxylase inhibitors for the treatment of renal anaemia and beyond. *Nat. Rev. Nephrol.* **12**, 157–168
8. Holdstock, L., Meadowcroft, A. M., Maier, R., Johnson, B. M., Jones, D., Rastogi, A., Zeig, S., Lepore, J. J., and Cobitz, A. R. (2016) Four-week studies of oral hypoxia-inducible factor-prolyl hydroxylase inhibitor GSK1278863 for treatment of anemia. *J. Am. Soc. Nephrol.* **27**, 1234–1244
9. Pergola, P. E., Spinowitz, B. S., Hartman, C. S., Maroni, B. J., and Haase, V. H. (2016) Vadadustat, a novel oral HIF stabilizer, provides effective anemia treatment in nondialysis-dependent chronic kidney disease. *Kidney Int.* **90**, 1115–1122
10. Higgins, D. F., Kimura, K., Bernhardt, W. M., Shrimanker, N., Akai, Y., Hohenstein, B., Saito, Y., Johnson, R. S., Kretzler, M., Cohen, C. D., Eckardt, K. U., Iwano, M., and Haase, V. H. (2007) Hypoxia promotes fibrogenesis in vivo via HIF-1 stimulation of epithelial-to-mesenchymal transition. *J. Clin. Invest.* **117**, 3810–3820
11. Baumann, B., Hayashida, T., Liang, X., and Schnaper, H. W. (2016) Hypoxia-inducible factor-1 α promotes glomerulosclerosis and regulates COL1A2 expression through interactions with Smad3. *Kidney Int.* **90**, 797–808
12. Li, Z. L., Lv, L. L., Tang, T. T., Wang, B., Feng, Y., Zhou, L. T., Cao, J. Y., Tang, R. N., Wu, M., Liu, H., Crowley, S. D., and Liu, B. C. (2019) HIF-1 α inducing exosomal microRNA-23a expression mediates the cross-talk between tubular epithelial cells and macrophages in tubulointerstitial inflammation. *Kidney Int.* **95**, 388–404
13. Debenham, J. S., Madsen-Duggan, C., Clements, M. J., Walsh, T. F., Kuethe, J. T., Reibarkh, M., Salowe, S. P., Sonatore, L. M., Hajdu, R., Milligan, J. A., Visco, D. M., Zhou, D., Lingham, R. B., Stickens, D., DeMartino, J. A., Tong, X., Wolff, M., Pang, J., Miller, R. R., Sherer, E. C., and Hale, J. J. (2016) Discovery of N-[Bis(4-methoxyphenyl)methyl]-4-hydroxy-2-(pyridazin-3-yl)pyrimidine-5-carboxamide (MK-8617), an orally active pan-inhibitor of hypoxia-inducible factor prolyl hydroxylase 1-3 (HIF PHD1-3) for the treatment of anemia. *J. Med. Chem.* **59**, 11039–11049
14. Yokoro, M., Nakayama, Y., Yamagishi, S. I., Ando, R., Sugiyama, M., Ito, S., Yano, J., Taguchi, K., Kaida, Y., Saigusa, D., Kimoto, M., Abe, T., Ueda, S., and Fukami, K. (2017) Asymmetric dimethylarginine contributes to the impaired response to erythropoietin in CKD-anemia. *J. Am. Soc. Nephrol.* **28**, 2670–2680
15. Kim, D. H., Marinov, G. K., Pepke, S., Singer, Z. S., He, P., Williams, B., Schroth, G. P., Elowitz, M. B., and Wold, B. J. (2015) Single-cell transcriptome analysis reveals dynamic changes in lncRNA expression during reprogramming. *Cell Stem Cell* **16**, 88–101
16. Liu, D., Wen, Y., Tang, T. T., Lv, L. L., Tang, R. N., Liu, H., Ma, K. L., Crowley, S. D., and Liu, B. C. (2015) Megalin/Cubulin-Lysosome-mediated albumin reabsorption is involved in the tubular cell activation of NLRP3 inflammasome and tubulointerstitial inflammation. *J. Biol. Chem.* **290**, 18018–18028
17. Liu, B. C., Tang, T. T., Lv, L. L., and Lan, H. Y. (2018) Renal tubule injury: a driving force toward chronic kidney disease. *Kidney Int.* **93**, 568–579
18. Meng, X. M., Nikolic-Paterson, D. J., and Lan, H. Y. (2016) TGF- β : the master regulator of fibrosis. *Nat. Rev. Nephrol.* **12**, 325–338
19. Shindo, T., Manabe, I., Fukushima, Y., Tobe, K., Aizawa, K., Miyamoto, S., Kawai-Kowase, K., Moriyama, N., Imai, Y., Kawakami, H., Nishimatsu, H., Ishikawa, T., Suzuki, T., Morita, H., Maemura, K., Sata, M., Hirata, Y., Komukai, M., Kagechika, H., Kadowaki, T., Kurabayashi, M., and Nagai, R. (2002) Krüppel-like zinc-finger transcription factor KLF5/BTEB2 is a target for angiotensin II signaling and an essential regulator of cardiovascular remodeling. *Nat. Med.* **8**, 856–863
20. Brigandi, R. A., Johnson, B., Oei, C., Westerman, M., Olbina, G., de Zoysa, J., Roger, S. D., Sahay, M., Cross, N., McMahon, L., Gupta, V., Smolyarchuk, E. A., Singh, N., Russ, S. F., and Kumar, S.; PHII12844

- Investigators. (2016) A novel hypoxia-inducible factor-prolyl hydroxylase inhibitor (GSK1278863) for anemia in CKD: a 28-day, phase 2A randomized trial. *Am. J. Kidney Dis.* **67**, 861–871
21. Chen, N., Qian, J., Chen, J., Yu, X., Mei, C., Hao, C., Jiang, G., Lin, H., Zhang, X., Zuo, L., He, Q., Fu, P., Li, X., Ni, D., Hemmerich, S., Liu, C., Szczec, L., Besarab, A., Neff, T. B., Peony Yu, K. H., and Valone, F. H. (2017) Phase 2 studies of oral hypoxia-inducible factor prolyl hydroxylase inhibitor FG-4592 for treatment of anemia in China. *Nephrol. Dial. Transplant.* **32**, 1373–1386
 22. Kimura, K., Iwano, M., Higgins, D. F., Yamaguchi, Y., Nakatani, K., Harada, K., Kubo, A., Akai, Y., Rankin, E. B., Neilson, E. G., Haase, V. H., and Saito, Y. (2008) Stable expression of HIF-1 α in tubular epithelial cells promotes interstitial fibrosis. *Am. J. Physiol. Renal Physiol.* **295**, F1023–F1029
 23. Sun, S., Ning, X., Zhang, Y., Lu, Y., Nie, Y., Han, S., Liu, L., Du, R., Xia, L., He, L., and Fan, D. (2009) Hypoxia-inducible factor-1 α induces Twist expression in tubular epithelial cells subjected to hypoxia, leading to epithelial-to-mesenchymal transition. *Kidney Int.* **75**, 1278–1287
 24. Grande, M. T., Sánchez-Laorden, B., López-Blau, C., De Frutos, C. A., Boutet, A., Arévalo, M., Rowe, R. G., Weiss, S. J., López-Novoa, J. M., and Nieto, M. A. (2015) Snail1-induced partial epithelial-to-mesenchymal transition drives renal fibrosis in mice and can be targeted to reverse established disease. *Nat. Med.* **21**, 989–997; erratum: 22, 217
 25. Baek, J. H., Zeng, R., Weinmann-Menke, J., Valerius, M. T., Wada, Y., Ajay, A. K., Colonna, M., and Kelley, V. R. (2015) IL-34 mediates acute kidney injury and worsens subsequent chronic kidney disease. *J. Clin. Invest.* **125**, 3198–3214
 26. Chen, W. C., Lin, H. H., and Tang, M. J. (2015) Matrix-stiffness-regulated inverse expression of Krüppel-Like Factor 5 and Krüppel-Like Factor 4 in the pathogenesis of renal fibrosis. *Am. J. Pathol.* **185**, 2468–2481
 27. Fujiu, K., Manabe, I., and Nagai, R. (2011) Renal collecting duct epithelial cells regulate inflammation in tubulointerstitial damage in mice. *J. Clin. Invest.* **121**, 3425–3441
 28. Higashi, A. Y., Aronow, B. J., and Dressler, G. R. (2019) Expression profiling of fibroblasts in chronic and acute disease models reveals novel pathways in kidney fibrosis. *J. Am. Soc. Nephrol.* **30**, 80–94
 29. Szeto, S. G., Narimatsu, M., Lu, M., He, X., Sidiqi, A. M., Tolosa, M. F., Chan, L., De Freitas, K., Bialik, J. F., Majumder, S., Boo, S., Hinz, B., Dan, Q., Advani, A., John, R., Wrana, J. L., Kapus, A., and Yuen, D. A. (2016) YAP/TAZ are mechanoregulators of TGF- β -Smad signaling and renal fibrogenesis. *J. Am. Soc. Nephrol.* **27**, 3117–3128
 30. Takeda, N., Manabe, I., Uchino, Y., Eguchi, K., Matsumoto, S., Nishimura, S., Shindo, T., Sano, M., Otsu, K., Snider, P., Conway, S. J., and Nagai, R. (2010) Cardiac fibroblasts are essential for the adaptive response of the murine heart to pressure overload. *J. Clin. Invest.* **120**, 254–265
 31. Kobayashi, H., Liu, Q., Binns, T. C., Urrutia, A. A., Davidoff, O., Kapitsinou, P. P., Pfaff, A. S., Olauson, H., Wernerson, A., Fogo, A. B., Fong, G. H., Gross, K. W., and Haase, V. H. (2016) Distinct subpopulations of FOXD1 stroma-derived cells regulate renal erythropoietin. *J. Clin. Invest.* **126**, 1926–1938
 32. Souma, T., Yamazaki, S., Moriguchi, T., Suzuki, N., Hirano, I., Pan, X., Minegishi, N., Abe, M., Kiyomoto, H., Ito, S., and Yamamoto, M. (2013) Plasticity of renal erythropoietin-producing cells governs fibrosis. *J. Am. Soc. Nephrol.* **24**, 1599–1616
 33. Ganz, T., and Nemeth, E. (2016) Iron balance and the role of hepcidin in chronic kidney disease. *Semin. Nephrol.* **36**, 87–93
 34. Provenzano, R., Besarab, A., Sun, C. H., Diamond, S. A., Durham, J. H., Cangiano, J. L., Aiello, J. R., Novak, J. E., Lee, T., Leong, R., Roberts, B. K., Saikali, K. G., Hemmerich, S., Szczec, L. A., Yu, K. H., and Neff, T. B. (2016) Oral hypoxia-inducible factor prolyl hydroxylase inhibitor roxadustat (FG-4592) for the treatment of anemia in patients with CKD. *Clin. J. Am. Soc. Nephrol.* **11**, 982–991
 35. Besarab, A., Chernyavskaya, E., Motylev, I., Shutov, E., Kumber, L. M., Gurevich, K., Chan, D. T., Leong, R., Poole, L., Zhong, M., Saikali, K. G., Franco, M., Hemmerich, S., Yu, K. H., and Neff, T. B. (2016) Roxadustat (FG-4592): correction of anemia in incident dialysis patients. *J. Am. Soc. Nephrol.* **27**, 1225–1233
 36. Haase, V. H. (2017) Therapeutic targeting of the HIF oxygen-sensing pathway: lessons learned from clinical studies. *Exp. Cell Res.* **356**, 160–165
 37. Paliege, A., Rosenberger, C., Bondke, A., Sciesielski, L., Shina, A., Heyman, S. N., Flippin, L. A., Arend, M., Klaus, S. J., and Bachmann, S. (2010) Hypoxia-inducible factor-2 α -expressing interstitial fibroblasts are the only renal cells that express erythropoietin under hypoxia-inducible factor stabilization. *Kidney Int.* **77**, 312–318
 38. Gerl, K., Miquero, L., Todorov, V. T., Hugo, C. P., Adams, R. H., Kurtz, A., and Kurt, B. (2015) Inducible glomerular erythropoietin production in the adult kidney. *Kidney Int.* **88**, 1345–1355
 39. Kalucka, J., Schley, G., Georgescu, A., Klanke, B., Rössler, S., Baumgartl, J., Velden, J., Amann, K., Willam, C., Johnson, R. S., Eckardt, K. U., and Weidemann, A. (2015) Kidney injury is independent of endothelial HIF-1 α . *J. Mol. Med. (Berl.)* **93**, 891–904
 40. Luo, R., Zhang, W., Zhao, C., Zhang, Y., Wu, H., Jin, J., Zhang, W., Grenz, A., Eltzschig, H. K., Tao, L., Kellems, R. E., and Xia, Y. (2015) Elevated endothelial hypoxia-inducible factor-1 α contributes to glomerular injury and promotes hypertensive chronic kidney disease. *Hypertension* **66**, 75–84
 41. Wang, L., Zhang, T., Fang, M., Shen, N., Wang, D., Teng, J., Fu, B., Xie, H., Hong, Q., and Lin, H. (2015) Podocytes protect glomerular endothelial cells from hypoxic injury via deSUMOylation of HIF-1 α signaling. *Int. J. Biochem. Cell Biol.* **58**, 17–27
 42. Hanna, C., Hubchak, S. C., Liang, X., Rozen-Zvi, B., Schumacker, P. T., Hayashida, T., and Schnaper, H. W. (2013) Hypoxia-inducible factor-2 α and TGF- β signaling interact to promote normoxic glomerular fibrogenesis. *Am. J. Physiol. Renal Physiol.* **305**, F1323–F1331

Received for publication April 28, 2019.
Accepted for publication July 30, 2019.